Available online at www.sciencedirect.com
ScienceDirect
Journal of Organometallic Chemistry 691 (2006) 4159–4166
Journal of Organometallic Chemistry
www.elsevier.com/locate/jorganchem

Study on DNA-binding properties and cytotoxicity in L_{1210} of La(III) complex with PMBP-isonicotinoyl hydrazone

Zheng-Yin Yang *, Bao-Dui Wang, Yan-Hua Li

School of Chemistry and Chemical Engineering and State Key Laboratory of Applied Organic Chemistry, Lanzhou University, Lanzhou 730000, PR China

Received 16 March 2006; received in revised form 24 May 2006; accepted 1 June 2006
Available online 15 June 2006

Abstract

La(III) complex with 1-phenyl-3-methyl-5-hydroxy-4-pyrazolyl phenyl ketone (PMBP)-isonicotinoyl hydrazone (La-complex) was synthesized in the work. The crystal of the La-complex was determined by X-ray diffraction analyses, the crystal of the complex is rhomb, space group R_3 with $Z = 6$, the coordination polyhedron of the complex is a tricapped triprism configuration with the nine-coordinate atoms, and the La-complex molecule looks like a helix structure according to its spacefill picture. Besides, it has been discovered that the La-complex possesses cytotoxic activities, and inhibitory rate for Leukemia cells (L_{1210}) is 87.1%. The interaction of the La-complex with DNA was investigated by absorption spectrum, fluorescence, CD spectrum and viscosity measurements. The DNA-binding constant for the La-complex is $(4.30 \pm 0.14) \times 10^6\ M^{-1}$.

Keywords: PMBP-isonicotinoyl hydrazone; La-complex; DNA-binding; Cytotoxic activities

1. Introduction

The DNA-binding metal complexes have been extensively studied as DNA structural probes, DNA-dependent electron transfer probes and so on during the past decade [1–5]. Although numerous biological experiments have also demonstrated that DNA is the primary intracellular target of anticancer drugs due to the interaction between small molecules and DNA, which can cause DNA damage in cancer cells, blocking the division of cancer cells and resulting in cell death [6–9], up to now the interaction of metal complexes with DNA is only tentative assessment for their potential biological and pharmaceutical activity, many problems still need to be elucidated for a better understanding of the mechanism and the biological implications of the interactions. One of the interesting questions is how the complex structure itself as well as the affinity and binding mode of DNA affects its pharmaceutical activities. The question answered will be of great advantage to establishing a potent way for selecting pharmaceutical compounds and exploring new antitumor drugs.

A great many Schiff base complexes with rare earths have provoked wide interest because of their diverse spectra of biological and pharmaceutical activities, such as anticancer, antitumor and antioxidative activities as well as the inhibition of lipid peroxidation, etc. PMBP-sonicotinoyl hydrazone (H_2L) constitute another class of Schiff bases ligand that has lately been shown able to form interesting complexes with lanthanides [10], and recent results have indicated that this type of ligand, when coordinating lanthanum (III), may improve biological and pharmaceutical activities of the complex due to forming special structure with lanthanum (III). It is unprecedented that a lanthanum (III) complex due to its pseudo helix structure appears some pharmaceutical activities. So the La-complex of the ligand is selected a target molecule which research the interaction with CT-DNA by absorption spectrum, fluorescence and viscosity measurements, and its crystal structure also has been determined by X-ray diffraction analyses in order

* Corresponding author. Tel.: +86 931 891 3515; fax: +86 931 891 2582.
E-mail address: yangzy@lzu.edu.cn (Z.-Y. Yang).

0022-328X/$ - see front matter © 2006 Elsevier B.V. All rights reserved.
doi:10.1016/j.jorganchem.2006.06.002

to investigate the pharmaceutical implications in the complex structure.

2. Results and discussion

2.1. Description of the crystal structure

The La-complex is a yellow, soluble in DMSO, methanol, slightly soluble in water, insoluble benzene and diethyl ether, can be kept in air for a long time. The molar conductivity of the complex is around 3.24 $ohm^{-1}\,cm^2\,mol^{-1}$ in ethanol, this shows that the La-complexes is a non-electrolytes in ethanol. The elemental analyses show the formula of the La-complexes, $C_{69}H_{62}LaN_{15}O_{10}$, with four H_2O for each complex confirmed by thermal analyses. The La-complex is an orange yellow crystal after crystallizing in an aqueous methanol (v/v = 1:1) solvent, X-ray diffraction analyses show that there are four lattice waters in each complex unit, $La(HL)_3 \cdot 4H_2O$ (see Fig. 1), the crystal of the complex is rhomb, space group R_3 with $Z = 6$, unit-cell dimensions $a = 19.3416(19)$ Å, $b = 19.3416(19)$ Å, $c = 33.955(7)$ Å, $\alpha = \beta = 90°$, and $\gamma = 120°$, $V = 11001(3)$ $Å^3$, $D_c = 1.268$ g/cm^3, $F(000) = 4338$, rhombohedral, $R\bar{3}$ $\mu(\text{Mo K}\alpha) = 0.646$ mm^{-1}, the final $R = 0.0451$. Some important bond lengths and bond angles are given in Tables 1 and 2, respectively. The data of C18–O2 (1.227 Å) and C1–O1 (1.264 Å) bond length in Table 1 show that the carbonyl 18 still are double bond, but carbonyl 1 almost turns a monobond in the complex, the C18–N4 is similar to double bond confirmed by C1–N1 (1.422 Å) > C18–N4 (1.331 Å) > C5 = N3 (1.305 Å), all of these demonstrate that the oxygens (O1) of carbonyl 1 take part in the coordination by the enolic form, and its active hydrogens are replaced by La(III), but ones(O2) of carbonyl 18 without the enolic form. The coordination polyhedron is a tricapped triprism configuration with the nine-coordinate atoms composed of three nitrogens and six oxygens from three ligands (HL) (see Fig. 2). The crystal is high symmetric rhomb with a principal axis, 3, of the symmetry. The La-complex looks like a helix structure according to spacefill structure (see Fig. 3).

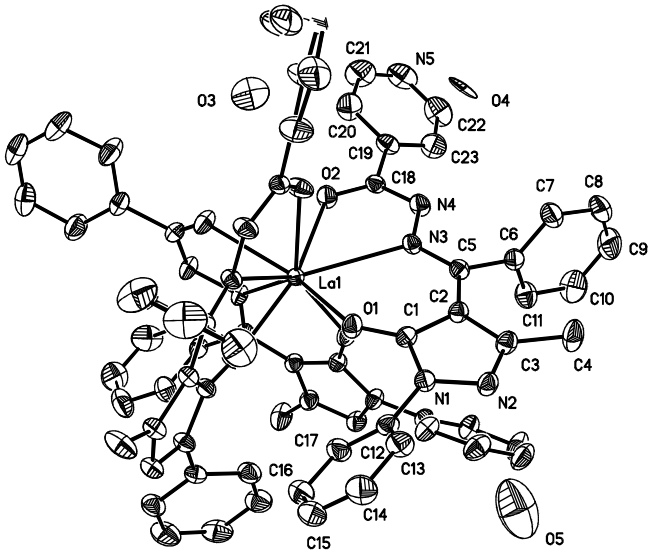

Fig. 1. Structure of La-complex.

2.2. Thermal analysis

Some data of thermal analyses are listed in Table 3. The DTA curves of the complexes have an endothermic peak between 86 and 90 °C, the corresponding TG curves show that the weight loss is equal to around four water molecules. These results are in accordance with the compositions of the complex determined by elemental analyses. Three exothermic peaks appear around 331–363, 458–478 and 528–547 °C, respectively. Initial temperature decomposed is greater than 330 °C, this indicates that thermal stability of the complexes are higher than that of the free ligand decomposed at 278 ° C, whose stability shows that there may be a large conjugation chelate ring exists in the complex.

2.3. Infrared spectra

The main stretching frequencies of the IR spectra of the ligand (H_2L) and the La-complex are tabulated in Table 4. The aqueous ν(OH) for the complex appears at 3350 cm^{-1}. $\nu(C^{18}{=}O)$ and $\nu(C^{1}{=}O)$ vibration of the free ligand are at 1616 and 1560 cm^{-1}, respectively, and corresponding peaks for the complex shift to 1602, 1434 cm^{-1}, $\Delta\nu$ is equal to 14, and 126 cm^{-1}, one of which ($C^1{=}O$) is similar to C—O due to the enolic form confirmed above the crystal structure analyses. δ_{NNH} vibrations of the free ligand at 1532 cm^{-1}, and the complex at 1539 cm^{-1} show that the active hydrogen of —NHN= group still exists in the complex. The band at 456 cm^{-1} is assigned to ν(M—O), all of these demonstrate that the oxygen of carbonyl has formed a coordinate bond with La(III). The band at 1588 cm^{-1} for the free ligand is assigned to the ν(C=N) stretch, it shifts to 1571 cm^{-1} for the complex, weak band at 405 cm^{-1} is assigned to ν(M—N). This further confirms that the nitrogen of imino-group bonds to La(III). All of these data confirm the fact that a conjugate chelate ring formed by ligand enolazition exists in the complex. This is consistent with the analysis results of the crystal structure of the La-complex.

2.4. Biological activities

2.4.1. Cytotoxic activities

Test results of the La-complex for KB, HCT-8, Bel7402, A2780 and L_{1210} cells are summarized in Table 5. Inhibitory rate of the La-complex for L_{1210} cells is 87.1%, but effects on other cells are minus. It is clear that the complex obviously affects L_{1210} cells, but both free ligand (H_2L) and lanthanum (III) are not able to affect L_{1210} cells. This shows that the cooperative effect between metal and ligand can improve the pharmaceutical activity

Table 1
Important data of bond lengths (Å)

Bond names	Bond lengths	Bond names	Bond lengths	Bond names	Bond lengths
La–O(1)1	2.382(3)	La–O(1)	2.382(3)	C(8)–C(9)	1.348(10)
La–O(1)2	2.3882(3)	La–O(2)	2.545(3)	C(10)–C(11)	1.386(8)
La–O(2)1	2.545(3)	La–N(3)1	2.821(3)	C(12)–C(13)	1.374(6)
La–O(2)2	2.545(3)	La–N(3)2	2.821(3)	C(12)–C(17)	1.396(6)
La–N(3)	2.821(3)	O(1)–C(1)	1.264(5)	C(13)–C(14)	1.382(7)
N(1)–C(1)	1.371(5)	O(2)–C(18)	1.227(5)	C(14)–C(15)	1.361(8)
N(1)–N(2)	1.386(5)	C(1)–C(2)	1.408(6)	C(15)–C(16)	1.372(8)
N(1)–C(1)2	1.422(5)	C(2)–C(3)	1.423(6)	C(16)–C(17)	1.367(7)
N(2)–C(3)	1.324(5)	C(2)–C(5)	1.433(5)	C(18)–C(19)	1.501(5)
N(3)–C(5)	1.305(5)	C(3)–C(4)	1.503(7)	C(19)–C(23)	1.360(7)
N(3)–C(4)	1.407(4)	C(5)–C(6)	1.498(6)	C(19)–C(20)	1.365(7)
N(4)–C(18)	1.331(5)	C(6)–C(11)	1.373(7)	C(20)–C(21)	1.383(8)
N(5)–C(21)	1.286(9)	C(6)–C(7)	1.378(6)	C(22)–C(23)	1.390(8)
N(5)–C(22)	1.317(9)	C(7)–C(8)	1.392(8)		
O(1)–C(1)	1.264(5)	C(9)–C(10)	1.366(10)		

Table 2
Important bond angles

Bond angles	Angle (°)	Bond angles	Angle (°)	Bond angles	Angle (°)
O(1)1–La–O(1)2	83.79(11)	O(1)1–La–N(3)2	142.30(10)	N(3)–C(5)–C(2)	120.2(4)
O(1)1–La–O(1)	83.79(11)	O(1)2–La–N(3)2	67.40(9)	N(3)–C(5)–C(6)	120.8(3)
O(1)2–La–O(1)	83.79(11)	O(1)–La–N(3)2	69.87(10)	C(2)–C(5)–C(6)	118.8(3)
O(1)1–La–O(2)	85.25(11)	O(2)–La–N(3)2	132.12(10)	C(11)–C(6)–C(7)	119.6(4)
O(1)2–La–O(2)	145.57(10)	O(2)1–La–N(3)2	75.78(10)	C(11)–C(6)–C(5)	117.9(5)
O(1)–La–O(2)	127.23(9)	O(2)2–La–N(3)2	60.36(9)	C(7)–C(6)–C(5)	122.5(4)
O(1)1–La–O(2)1	127.23(9)	N(3)1–La–N(3)2	119.89(7)	C(6)–C(7)–C(8)	119.3(5)
O(1)2–La–O(2)1	85.25(11)	N(3)–La–N(3)2	119.89(7)	C(9)–C(8)–C(7)	120.9(6)
O(1)–La–O(2)1	145.57(10)	C(1)–N(1)–N(2)	111.9(3)	C(8)–C(9)–C(10)	120.0(6)
O(2)–La–O(2)1	75.76(11)	C(1)–N(1)–C(12)	127.4(3)	C(9)–C(10)–C(11)	120.1(6)
O(1)1–La–O(2)2	145.57(10)	N(2)–N(1)–C(12)	120.4(3)	C(6)–C(11)–C(10)	120.0(5)
O(1)2–La–O(2)2	127.23(9)	C(3)–N(2)–N(1)	105.3(3)	C(13)–C(12)–C(17)	119.5(4)
O(1)–La–O(2)2	85.25(11)	C(5)–N(3)–N(4)	114.2(3)	C(13)–C(12)–N(1)	120.7(4)
O(2)–La–O(2)2	75.76(11)	C(5)–N(3)–La	131.7(2)	C(17)–C(12)–N(1)	119.8(4)
O(2)1–La–O(2)2	75.76(11)	N(4)–N(3)–La	110.6(2)	C(12)–C(13)–C(14)	119.5(5)
O(1)1–La–N(3)1	67.40(9)	C(18)–N(4)–N(3)	119.2(3)	C(15)–C(14)–C(13)	120.6(5)
O(1)2–La–N(3)1	69.87(10)	C(21)–N(5)–C(22)	117.1(5)	C(14)–C(15)–C(16)	120.5(5)
O(1)–La–N(3)1	142.30(10)	C(1)–O(1)–La	139.1(3)	C(17)–C(16)–C(15)	119.7(5)
O(2)–La–N(3)1	75.78(10)	C(18)–O(2)–La	125.0(2)	C(16)–C(17)–C(12)	120.2(5)
O(2)1–La–N(3)1	60.36(9)	O(1)–C(1)–N(1)	122.0(4)	O(2)–C(18)–N(4)	123.8(4)
O(2)2–La–N(3)1	132.12(10)	O(1)–C(1)–C(2)	132.1(4)	O(2)–C(18)–C(19)	120.3(4)
O(1)1–La–N(3)	69.87(10)	N(1)–C(1)–C(2)	105.9(3)	N(4)–C(18)–C(19)	115.9(4)
O(1)2–La–N(3)	142.30(10)	C(1)–C(2)–C(3)	105.1(3)	C(23)–C(19)–C(20)	117.3(5)
O(1)–La–N(3)	67.40(9)	C(1)–C(2)–C(5)	124.9(4)	C(23)–C(19)–C(18)	123.9(4)
O(2)–La–N(3)	60.36(9)	C(3)–C(2)–C(5)	129.9(4)	C(20)–C(19)–C(18)	118.7(4)
O(2)1–La–N(3)	132.12(10)	N(2)–C(3)–C(2)	111.7(4)	C(19)–C(20)–C(21)	118.6(6)
O(2)2–La–N(3)	75.78(10)	N(2)–C(3)–C(4)	117.6(4)	N(5)–C(21)–C(20)	124.7(6)
N(3)1–La–N(3)	119.89(8)	C(2)–C(3)–C(4)	130.7(4)	N(5)–C(22)–C(23)	122.5(6)

of the metal complex. Acute toxicity data (LD_{50}) of the La-complex is 348.9 ± 32 mg kg^{-1}, whose toxicity is not remarkable. Although the mechanism which the La-complex selectively affects L_{1210} is still unclear, its special structure is vital. Lots of other heterocyclic Schiff's bases Lanthanum complexes often appear similar biological and pharmaceutical activities, for example, Lanthanum complexes with both 4′,5,7-trihydroxy-flavanoe benzoyl hydrazone [11] and phthalazin-1(2H)-one [12] have considerable cytotoxic activity against two kinds of tumor cells (human leukemia HL-60 and lung adenocarinoma A-549), the two complexes can strongly bind with calf thymus DNA, the intrinsic binding constants of their complexes with DNA are 1.83×10^7 and 1.4×10^7 M^{-1}, respectively. This is an interesting phenomenon, which also show that the interaction between the complex molecules and DNA can cause DNA damage in tumor cells, blocking the division of tumor cells and resulting in the cell death [8,9]. So DNA-binding properties of the La-complex will be discussed as follows.

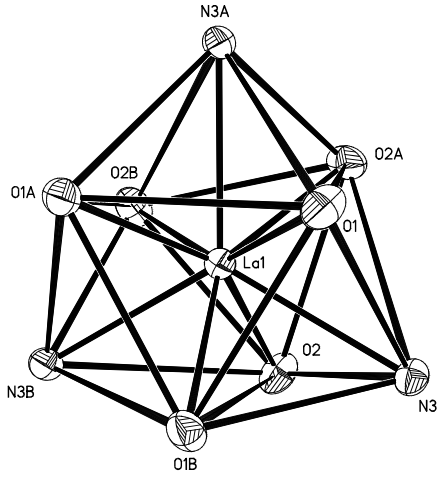

Fig. 2. The coordination polyhedron.

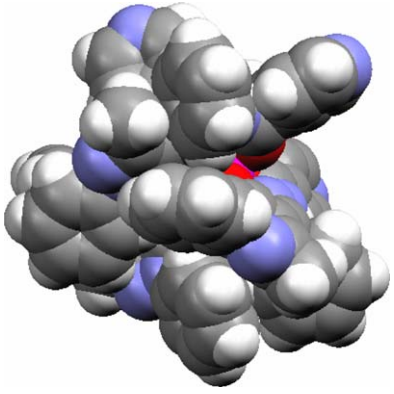

Fig. 3. Spacefill structure of La-complex.

2.4.2. UV–Vis absorption spectroscopy

The absorption spectra of the ligand and the La-complex in the absence or presence of DNA are shown in Fig. 4(a) and (b), respectively. With increasing DNA concentrations, the absorption bands at 202, 247 and 386 nm for the ligand appear hypochromism of 27.65%, 2.67% and 50%, the absorption bands at 203, 256 and 388 nm for the La-complex also appear different hypochromism of 54.47%, 43.91% and 31.62%. The hypochromism observed for the $\pi \rightarrow \pi^*$ transition bands of ligand at 202 nm and the La-complex at 203 nm are accompanied by a 2 and 14 nm red-shift, it is clear that the hypochromism and the red-shift are not enough evidence. When the molecular size and the pseudo helix structure of the La-complex are considered, the interaction mode with DNA may be a groove binding. After the La-complex binds to the base pairs of DNA, the π^* orbital of the intercalated the ligand could couple with π orbit of the base pairs, thus, decreasing the $\pi \rightarrow \pi^*$ transition energies. On the other hand, the coupled π^* orbital is partially filled by electrons, thus decreasing the transition probabilities. Thus, these effects result in the hypochromism and bathochromism [13]. The La-complex shows somewhat more hypochromisims than the ligand, indicating that the La-complex intercalate into DNA more strongly than ligand does.

2.4.3. Luminescence studies

The ligand and the La-complex can luminescence in Tris buffer at room temperature with maximum at 452 and 458 nm, respectively. Upon addition of DNA, the emission intensities of the compounds grow to around 1.26 times for

Table 3
Thermal analyses data of the complexes

Complex	D[a] T °C	M.p. T °C	Process	%H_2O loss		Decomposed			Process	Residue
				Calc.	Found	T_1	T_2	T_3		
H_2L		243	Endothermic			278	395	543	Exothermic	
$La(HL)_3 \cdot 4H_2O$	87		Endothermic	4.52	5.1	352	458	528	Exothermic	La_2O_3

[a] D = dehydration.

Table 4
Some main IR data of the ligand and the La-complex

Complexes	ν_{OH}	ν_{NH}	$\nu_{C^{18}=O}$	$\nu_{C=N}$	$\nu_{C^1=O}$	δ_{HOH}	δ_{NNH}	ν_{M-O}	ν_{M-N}
H_2L		3058m	1616m	1588w	1560s		1532m		
$La(HL)_3 \cdot 4H_2O$	3353m	3051m	1602m	1571w	1434s	1638s	1539s	456w	405w

Table 5
Test results of inhibitory tumor cells out body

Complex	Test cells	Dose (μg/ml)	Effects	Results	Inhibitory rate (%)
$La(HL)_3 \cdot 3.5H_2O$	KB	10, 1	>10	−	
	HCT-8	10, 1	>10	−	
	Be17402	10, 1	>10	−	
	A2780	10, 1	>10	−	
	L1210	10, 1	<10	+	87.1, 32.4
H_2L, $LaCl_3$	L1210	10, 1	>10	−	

'Effects' means that the tested complex whose dose is less than 10 μg/mL appear the result of inhibitory for the tested cells; 'Results' means the result of 'Effects', '+' having inhibitory, '−' no inhibitory; inhibitory rate = 100% (control group − test group)/control group.

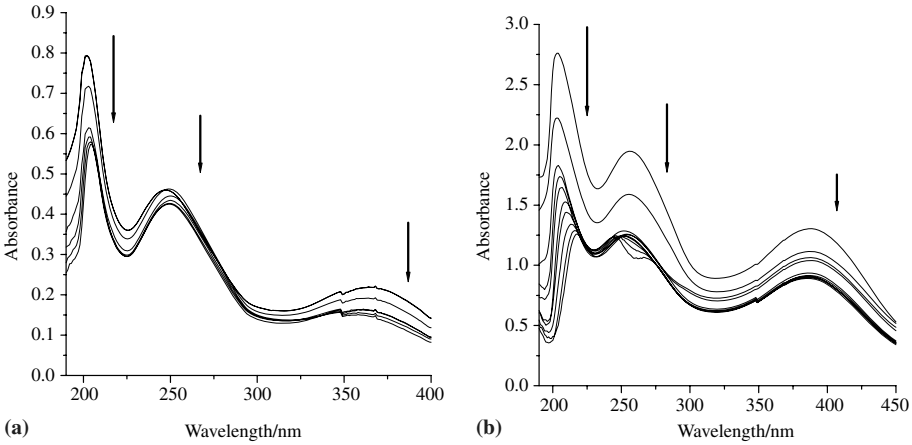

Fig. 4. (a) Electronic spectra of the ligand (10 μM) in the presence of CT-DNA. [DNA] = 0–25 μM. Arrow shows the absorbance changes upon increasing DNA concentration. (b) Electronic spectra of the La-complex (10 M) in the presence of CT-DNA. [DNA] = 0–40 μM. Arrow shows the absorbance changes upon increasing DNA concentration.

the ligand and 1.32 times for the La-complex as shown in Fig. 5. The magnitudes of emission enhancement for the La-complex are much larger than that for the ligand, therefore we can also infer that the La-complex inserts more deeply into DNA than the ligand does. According to the Scatchard equation, a plot of r/C_f versus r gives the binding constants $(1.99 \pm 0.046) \times 10^6$ and $(4.30 \pm 0.14) \times 10^6$ M^{-1} from the fluorescence data for the ligand and the La-complex, respectively. The results show that the complex binds more strongly than the ligand. The higher binding affinity of the La-complex is probably relate to its pseudo helix structure (see Fig. 3) since the structure of the La-complex is able to provide lots of grooving positions to stack more strongly with the base pairs of the DNA helix.

The emission spectra of DNA-bound EB in the absence and the presence of the ligand and the La-complex are given in Fig. 6. The addition of the ligand and the La-complex to the DNA-bound EB solutions cause obvious reduction in emission intensities, indicating that the ligand and the La-complex competitively bind to DNA and

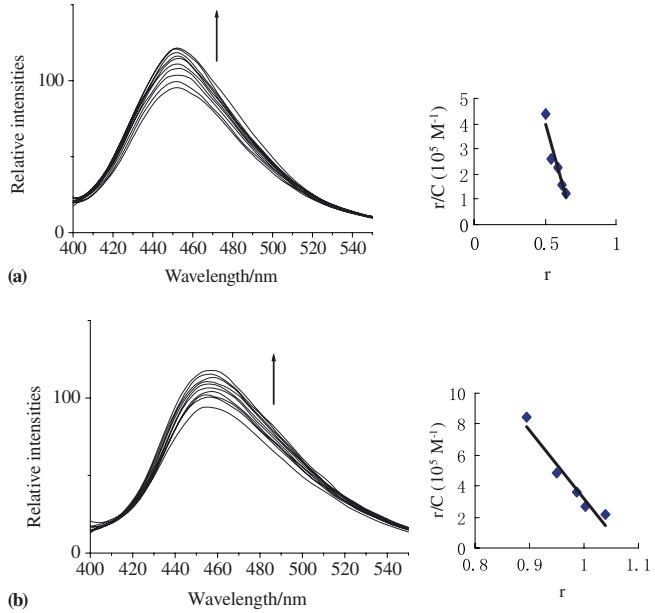

Fig. 5. (a) The emission enhancement spectra of the ligand (10 μM) in the presence of 0, 2.5, 5, 7.5, 10, 12.5, 15, 17.5, 20 μM CT-DNA. Arrow shows the emission intensities changes upon increasing DNA concentration. Inset: Scatchard plot of the fluorescence titration data of the ligand, $K = (1.99 \pm 0.046) \times 10^6$ M^{-1}. (b) The emission enhancement spectra of the La-complex (10 μM) in the presence of 0, 1.25, 2.50, 3.75, 5.00, 6.25, 7.50, 8.75, 10.0 and 11.25 μM CT-DNA. Arrow shows the emission intensities upon increasing DNA concentration. (Inset) Scatchard plot of the fluorescence titration data of the La-complex, $K = (4.30 \pm 0.14) \times 10^6$ M^{-1}.

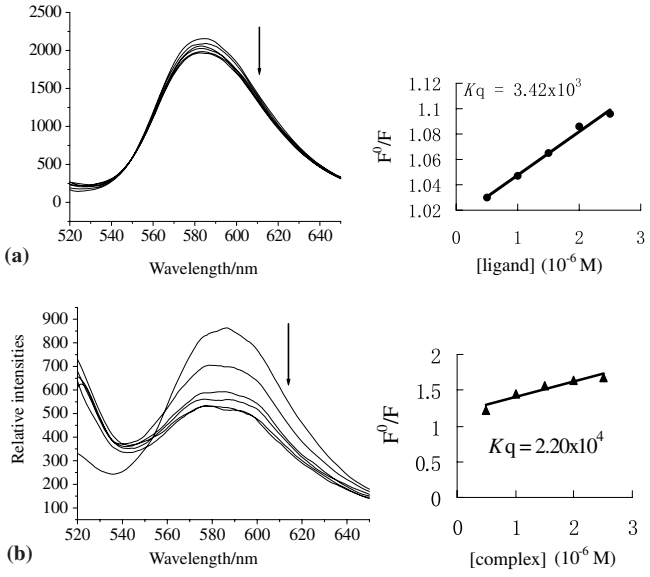

Fig. 6. (a) The emission spectra of calf thymus DNA-EB system (10 μM and 0.32 μM EB), $\lambda_{ex} = 500$ nm, $\lambda_{em} = 520.0$–650.0 nm, in the presence of 0, 5, 10, 15, 20, 25, 30 μM the ligand. Arrow shows the emission intensities changes upon increasing ligand concentration. (Inset) Stern–Volmer plot of the fluorescence titration data of ligand, $K_q = 3.42 \times 10^3$ M^{-1}. (b) The emission spectra of DNA-EB system (10 μM and 0.32 μM EB), $\lambda_{ex} = 500$ nm, $\lambda_{em} = 520.0$–650.0 nm, in the presence of 0, 5, 10, 15, 20, 25, 30 μM the La-complex. Arrow shows the emission intensities changes upon increasing the La-complex concentration. (Inset) Stern–Volmer plot of the fluorescence titration data of the La-complex, $K_q = 2.20 \times 10^4$ M^{-1}.

displace bound EB. The quenching plots illustrate that the quenching of EB bound to DNA by the ligand and the complex are in good agreement with the linear Stern–Volmer equation. In the plots of F_0/F versus $[Q]$, the quenching plots of system EB-DNA by successive addition of the compounds give linear Stern–Volmer equation with K_q values of 3.42×10^3 M^{-1} for the ligand and 2.20×10^4 M^{-1} for the La-complex. This shows that the binging interaction of the complex with DNA more strongly than that of the ligand.

2.4.4. Viscosity measurements

Though optical photophysical probes generally provide necessary clues, it is not enough to confirm binding mode. To clarify the nature of the interaction between the compounds and DNA, the changes in the specific relative viscosities of DNA upon addition of the compounds have to be examined (see Fig. 7). The viscosity of a DNA solution is sensitive to the addition of the ligand and the La-complex bound by intercalation mode. The viscosities of DNA bound to the compounds increase with the increment of the concentrations of the compounds, and changes in the viscosities caused by the complex are more evident than by ligand. The experimental results show that the La-complex intercalated between the two adjacent base pairs of DNA through a non-classical intercalation mode [14,15], and the La-complex binds to the DNA more tightly than the ligand. The results obtained from viscosity studies validate those obtained from spectroscopic studies. So the intercalation mode include bath intercalation and grooving.

2.4.5. CD spectroscopy

CD spectral technique is useful in monitoring the conformational variations of DNA in solution. The CD spectra of CT-DNA upon addition of the La-complex are showed in Fig. 8. Both the plus (~275 nm) and the minus (~245 nm) bands increased in intensity upon addition of the La-complex to DNA. This phenomenon may be due to the intercalation of the complex through p-stacking which stabilizes the right-handed B form DNA [16].

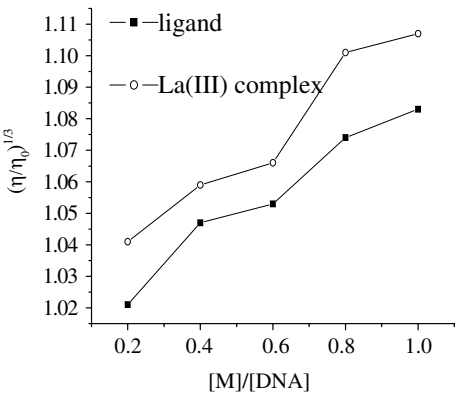

Fig. 7. Effect of increasing amounts of the La-complex and the ligand on the relative viscosity of calf thymus DNA at 25.0 °C.

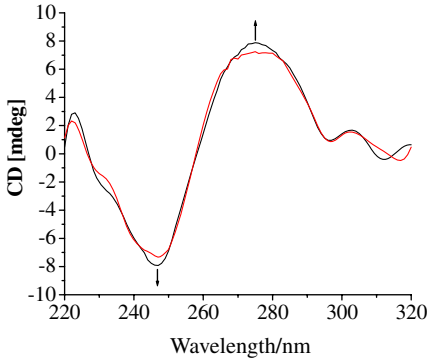

Fig. 8. CD spectra of CT DNA (1.0×10^{-4} M) at $1/R$ (La-complex)/[DNA] value of 0.5: (···) the absence of La-complex; (—) the presence of La-complex.

2.5. Conclusion

On the basis of the spectroscopic, the viscosity and the structure studies of the complex, it comes to the conclusion that the La-complex and the ligand can bind to CT-DNA by both intercalative and groove mode, that the La-complex binds to CT-DNA more strongly than ligand, which the intrinsic binding constant for the ligand and the La-complex are $(1.99 \pm 0.046) \times 10^6$ and $(4.30 \pm 0.14) \times 10^6$ M^{-1}, respectively. K of DNA with other Schiff base metal complexes, ligand derived from methyl salicylal D-glucamine [17], 4′,5,7-trihydroxy-flavanoe benzoyl hydrazone [11] and phthalazin-1(2H)-one [12], are about 10^5–10^7 M^{-1}. The La-complex inhibitory rate for L_{1210} cells is 87.1%, but the ligand and the La(III) are not able to affect L_{1210} cells. It is clear that pharmaceutical activities of the La-complex are improved due to both the cooperative effect of the metal with the ligand and the pseudo helix structure of the complex. So the higher binding affinity of the La-complex with DNA probably implicates its pharmaceutical activities.

3. Experimental

3.1. Materials

Calf thymus DNA and ethidium bromide (EB) were purchased from Sigma (USA). 1-Phenyl-3-methyl-4-benzoyl-5-pyrazolone(PMBP) and isoniazid were produced of China. The lanthanum(III) chlorides was prepared by dissolving La_2O_3 (Nong Hua in China) in concentrated HCl, then crystallizing the products. EDTA-Fe(II) and KH_2PO_4–K_2HPO_4 buffers were prepared by deionized water. All chemicals used were of analytical grade.

3.2. Physical measurements

Carbon, hydrogen and nitrogen were analyzed on a Vario EL elemental analyzer. Infrared spectra (4000–400 cm^{-1}) were obtained with KBr discs on a Therrno Mattson FTIR spectrometer. ^1H NMR spectra were measured on a Varian Mercury Plus 300 BB, using TMS

as an internal standard in DMSO-d_6. The thermal behavior was monitored on a PCT-2 differential thermal analyzer. The ultraviolet spectra were recorded on a Shimadzu UV-240 spectrophotometer. Fluorescence measurements were determined at room temperature using a Hitachic RF-540 spectrofluorophotometer equipped with quartz cuvettes of 1 cm path length. Above-mentioned experiments involving the interaction of the ligand and the complex with CT-DNA were carried out in a mixture solvent of CH_3OH (1%) and doubly distilled water buffer containing 5 mM Tris and 50 mM NaCl and adjusted to pH 7.1 with hydrochloric acid. In order to eliminate the absorbance of nucleic acid itself, an equal amount of CT-DNA was added into the sample and the reference cell, respectively. Spectrometric titrations, ethidium bromide displacement experiments and viscosity measurement were performed as according to Refs. [18,19].

The CD spectra were recorded on a Olos RSM 1000 at room temperature at increasing complex/CT-DNA ratio ($r = 0.0$, 0.5). Each sample solution was scanned in the range of 220–320 nm. A CD spectrum was generated which represented the average of three scans from which the buffer background had been subtracted. The concentration of CT-DNA was 1.0×10^{-4} M.

A orange yellow crystal of the La-complex ($0.46 \times 0.41 \times 0.29$ mm) was mounted on a Bruker Smart-1000 CCD diffractometer, and determined with graphite monochromated Mo Kα radiation (0.71073 Å). Intensities were measured using $\theta/2\theta$ scan technique, 2θ range: 3.42–50.04°, ($h = -21$ to 23, $k = -23$ to 18, $l = -34$ to 40); 19 186 unique reflections were collected at 295(2) K, 4278 observed [$I > 3\sigma(I)$] of which were used to solve the structure and least-square refinement. The data of diffraction were corrected by the LP factor, absorption correction was made by semi-empirical psi-scans. The La atom was located from a Patterson's function and the other non-hydrogen atoms from Fourier synthesis. The structure was refined with full-matrix least-square on F^2, all hydrogen atoms were located from a difference-Fourier synthesis. The final R factor was equal to 0.0455 ($R_2 = 0.1261$).

3.3. Preparation of the ligand

The ligand, 1-phenyl-3-methyl-5- hydroxy-4-pyrazolyl phenyl ketone (PMBP)-isonicotinoyl hydrazone (H_2L), was prepared in ethanol by refluxed on a water bath [10], m.p.244–245 °C. Anal. Calc. for $C_{23}H_{19}N_5O_2$: C, 69.50; H, 4.82; N, 17.26. Found: 69.43; H, 4.89; N, 17.08%. ^{1}H NMR (DMSO-d_6), δ (ppm): 1.50 (3H, singlet, CH_3); 7.10–7.90 (11H, multiplet, 2 phenyl, –NH–); 8.20 (2H, doublet, $J = 6$ Hz, H^3, H^5 of pyridine ring); 8.76 (2H, broad, H^2, H^6 of pyridine ring).

3.4. Preparation of the complex

Ligand H_2L (2 mmol) was added to water (40 mL), the pH of which was adjusted to 7 by the addition of an aqueous solution of NaOH (10%), the solution turned light yellow. Then a solution of $LaCl_3 \cdot 6H_2O$ (1 mmol) in water (10 mL) was added dropwise to the system. After stirring at 50 °C for 0.5 h a yellow precipitate was separated by filtration, purified by washing with water, and heated ethanol, respectively, and dried in a vacuum, 20 mg of the La-complex was dissolved in 20 ml of an aqueous methanol (v/v = 1:1) solvent, the solution was filtrated, the resulting solution was diluted to 40 mL with water. After crystallizing by spontaneous evaporation at room temperature for a week, the crystalline complex was separated the solution. Anal. Calc. for $C_{69}H_{62}LaN_{15}O_{10}$: C, 58.77; H, 4.47; N, 14.79; La, 10.70. Found: C, 58.46; H, 4.38; N, 14.54; La, 10.31%.

3.5. Biological and pharmacological test

The interaction of the La-complex with DNA was investigated by absorption spectrum, fluorescence and viscosity measurements [11,12]. Absorption titration experiment was performed with fixed concentrations of the drugs (20 μM) while gradually increasing concentration of DNA. An excitation wavelength of 352 nm was used, and total fluorescence emission intensity was monitored at 446 nm, which fixed amounts of compound were titrated with increasing amounts of DNA, over a range of DNA concentrations from 3.0 to 40.0 μM. Viscosity experiments were conducted on an Ubbdlodhe viscometer, immersed in a thermostated water-bath maintained to 25.0 °C.

The CD spectra were recorded at room temperature by increasing complex/CT-DNA ratio ($r = 0.0$, 0.5). Each sample solution was scanned in the range of 220–320 nm. A CD spectrum was generated which represented the average of three scans from which the buffer background had been subtracted. The concentration of CT-DNA was 1.0×10^{-4} M.

Inhibitory tests on tumor cells were performed as according to Ref. [20]. Tumour cells (1×10^3/ml), the tested complexes (1.0×10^{-5}–1.0×10^{-3} μg ml^{-1}), 20% FCS and RPMI-1640 medium were mixed thoroughly. Then 3% agar–agar was added into the mixture as supporting material to the final concentration of 0.3%, next the mixture was immediately inoculated on a 35 mm culture dish and cultivated for 5 days at 37 °C, 5% CO_2 and saturated humidity incubator. The lines, contained 50 cells, were counted under an inverted microscope.

Acknowledgments

Project is supported by National Natural Science Foundations in China (20475023) and Gansu NSF (3ZS041-A25-016), and inhibitory tumor cells were tested by Chinese Academy of Medical Sciences. We are grateful to D.Q. Wang for solving the crystal structure.

Appendix A. Supplementary data

Supplementary data associated with this article can be found, in the online version, at doi:10.1016/j.jorganchem.2006.06.002.

References

[1] B.Y. Wu, L.H. Gao, Z.M. Duan, K.Z. Wang, J. Inorg. Biochem. 99 (2005) 1685.
[2] K.E. Erkkila, D.T. Odom, J.K. Barton, Chem. Rev. 99 (1999) 2777.
[3] C. Metcalfe, J.A. Thomas, Chem. Soc. Rev. 32 (2003) 215.
[4] I. Haq, P. Lincoln, D. Suh, B. Norden, B.Z. Choedhry, J.B. Chaires, J. Am. Chem. Soc. 117 (1995) 4788.
[5] S. Arturo, B. Giampaolo, R. Giuseppe, L.G. Maria, T. Salvatore, J. Inorg. Biochem. 98 (2004) 589.
[6] N. Maribel, C.F. Efrén, S. Anßbal, F.M. Mercedes, S. Pedro, A. Dwight, M. Edgar, J. Biol. Inorg. Chem. 8 (2003) 401.
[7] H. Catherine, P. Marguerite, R.G. Michael, S. Stéphanie Heinz, M. Bernard, J. Biol. Inorg. Chem. 6 (2001) 14.
[8] V.S. Li, D. Choi, Z. Wang, L.S. Jimenez, M.S. Tang, H. Kohn, J. Am. Chem. Soc. 118 (1996) 2326.
[9] G. Zuber, J.C. Quada Jr., S.M. Hecht, J. Am. Chem. Soc. 120 (1998) 9368.
[10] Z.Y. Yang, R.D. Yang, Q. Li, F.S. Li, Syn. React. Inorg. Metal–Org. Chem 29 (1999) 205.
[11] B.D. Wang, Z.Y. Yang, Q. Wang, C.T. Kuan, P. Crewdson, Bioorg. Med. Chem. 14 (2006) 1880.
[12] Y. Wang, Z.Y. Yang, Q. Wang, J. Org.-Met.Chem. 690 (2005) 4557.
[13] S.M. Hecht, J. Nat. Prod. 63 (2000) 158.
[14] Y. Xiong, X.F. He, X.H. Zou, J.Z. Wu, X.M. Chen, L.N. Ji, R.H. Li, J.Y. Zhou, R.B. Yu, J. Chem. Soc., Dalton Trans. 1 (1999) 19.
[15] S. Satyanarayana, J.C. Dabrowiak, J.B. Chaires, Biochemistry 32 (1993) 2573.
[16] P.U. Maheswari, M. Palaniandavar, J. Inorg. Biochem. 98 (2004) 219.
[17] Y.H. Huang, H.Y. Sheng, S. Long, Chem. Bull. 56 (2002) 1.
[18] S. Satyanarayana, J.C. Dabrowiak, J.B. Chaires, Biochemistry 31 (1992) 9319.
[19] Y. Wang, Z.Y. Yang, Trans. Metal Chem. 30 (2005) 902.
[20] Z.Y. Yang, L.F. Wang, X.P. Yang, D.W. Wang, Y.M. Li, J. Rare Earth 2 (2000) 140.